RSC Advances

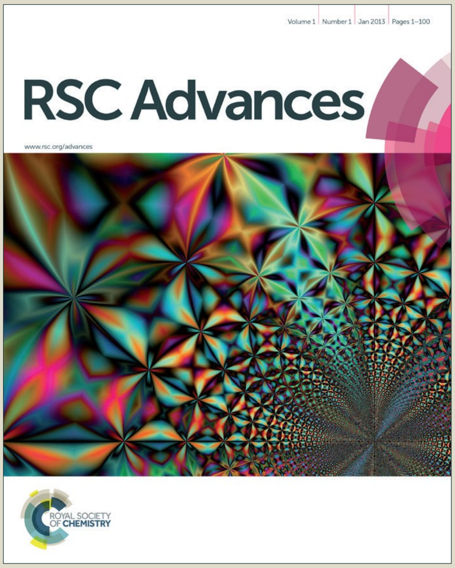

ROYAL SOCIETY OF CHEMISTRY

www.rsc.org/advances

Synthesis and Characterization of low specific resistance alumina-clay-carbon composites by colloidal processing using sucrose as a soluble carbon source for electrical applications

Rahul Kumar, Parag Bhargava*

Department of Metallurgical Engineering and Materials Science
Indian Institute of Technology Bombay, Mumbai, India 400076,

Email- pbhargava@iitb.ac.in

Abstract

Switching resistors in high voltage circuit breakers require use of materials with low specific resistance which can sustain high temperatures for short durations, have high thermal conductivity and thermal shock resistance. Materials that satisfy these requirements can be produced by dispersing a conducting phase such as carbon black, graphite, CNT, graphene in ceramic matrix. Dispersion of these ultrafine forms of carbon to obtain contiguity at lower volume fractions is a challenge. In this work, alumina-clay-carbon composites were fabricated by using alumina-clay slurries with addition of sucrose as a soluble carbon source. Sucrose is converted into conducting carbon with heat treatment at high temperature. Alumina-clay-carbon composites made by soluble source (sucrose) sintered at 1400^{o}C showed resistor behaviour even at carbon content less than 1 wt % produced by graphitization of sucrose at high temperature. Raman spectroscopic scans over a wide area of the samples confirmed uniform distribution of carbon within the ceramic matrix. Resistivity of the alumina-clay-carbon composites varied between 30 Ohm-cm to 2 Ohm-cm for sucrose addition (equivalent carbon content) of 2 – 9wt %. The resistivity of the composite samples produced with use of sucrose was significantly lower than that of samples produced by dispersing carbon black as the conducting phase.

Key words: Alumina-clay-carbon composites; Colloidal processing; Electrical properties; Thermal properties; Mechanical properties

1. Introduction

From the perspective of electrical insulation, ceramic materials are among the best insulators with resistivity at room temperature exceeding 10^{14} ohm-cm. There are applications that require use of ceramic materials that have low resistivity such that these materials can allow passage of large electrical currents and yet sustain high temperatures. Also, these materials must have high thermal conductivity in order to sustain thermal shock. High voltage linear resistors are one such application which requires these materials to have the capability of handling energies ranging from Joules to Mega-Joules, at frequencies up to Mega-Hz. These high voltage resistors can be used in applications such as electrical transmission, traction, AC/DC drives, pulse power, dummy loads, induction heating and pulse forming networks [1]. Besides appropriately doping ceramic materials, resistivity of ceramic materials can be lowered by dispersing a conducting phase in amounts that results in contiguity of the conducting phase in three dimensions or formation of a percolating network [2-6]. Processing of ceramics with electrically conducting phase dispersed into the matrix has been undertaken through both dry and wet powder processing [7-12]. While it can be a challenge to disperse ultrafine particles in dry powder processing, it is relatively easier to achieve dispersion of ultrafine particles in the wet state, by breaking down agglomerates and promoting adsorption of dispersant molecules from solution which ensures that the particles remain deagglomerated.

Ceramic composites with dispersed conductive particles can be prepared from slurries either by compaction of spray dried granules produced from the slurries or by slipcasting or gelcasting of the slurries [13-18]. The percolation threshold of the fillers depends upon their physical characteristics such as particle size and aspect ratio. For low aspect ratio fillers such as carbon black and graphite, assuming a particle size of 2-5µm, the amount to be added was found to be at least 20 vol%, whereas the amount of additive required to achieve percolation with high-aspect-ratio carbon nanotubes (CNTs) was reduced to less than 12 vol% [19-23]. Indeed, it is not optimal for the conductive filler such as carbon to occupy a large volume of the ceramic matrix since it inevitably leads to degradation of the intrinsic structural properties of the host ceramics either due to non-homogeneous dispersion of the conductive filler or due to inhibited densification [24].

In one of the studies, the electrical resistivity of pure alumina sintered in an oxygen atmosphere at 1500^0C was found to be around 10^{12} Ohm-cm [25].The bulk resistivity of a sample sintered at 1600^oC under inert environment produced from alumina powder mixed with 1.4 vol% of carbon nanotubes by mechanical mixing was found to be 2000 Ohm-cm. A much lower resistivity was expected for a continuous carbon network but the relatively high value obtained indicated poor connectivity of the carbon phase. [26]. A. Bondar and Iordache [27] have reported lowered electrical resistivity values of 10^5 Ohm-cm for incorporation of 16 vol% graphite and 100 Ohm-cm for incorporation of 30 vol% graphite for sintered alumina samples produced from compaction of spray dried granules. Incorporation of 1.16 vol% to 11 vol% of carbon nanotube in alumina matrix lowered the resistivity of the composite from 250 Ohm-cm to 0.10 Ohm-cm [28] but the material was non-homogeneous due to challenges with dispersion and presence of agglomerates. So, there is a need of facile methods to produce composites with homogeneously dispersed conducting (carbon) phase with low electrical resistivity at as low a carbon amount as possible. Gel casting technique has shown some promise in this regard with gelcast alumina samples demonstrating resistivity of 2 Ohm-cm (for 10.75 wt % carbon) with uniformly distributed carbon. The uniform distribution of carbon phase was due to the pyrolysis of the in-situ polymer network obtained from soluble monomers added at the time of slurry preparation. The gelcast samples when sintered under inert environment contained continuous and homogeneous interlinking pathways of nano scale carbon as produced by pyrolysis of precursors [29]. The only limitation of the gelcasting process is the need to heat treat the samples to much higher temperatures, as compared to the case when a form of carbon (carbon black, graphite carbon nanotubes, graphene etc.) is added externally, above 1600^oC to convert the polymer network into graphitic state [30-33]. The present work addresses the need of developing a simpler method for obtaining uniformly dispersed carbon phase in ceramic matrix with low electrical resistivity.

2. Experimental work

2.1 Fabrication of alumina-clay-carbon composites

Alumina-clay-carbon composites were prepared using sucrose as a soluble source of carbon by slip casting as per flow chart shown in fig1. Sucrose (GR-Merck) was added to the PVA (S-D fine chemical, Molecular weight,125,000) solution containing 26 volume % ceramic (alumina-clay in 35: 65 wt. ratio, alumina HIM 30, Hindalco, clay, English India Clay, Kerala) in amounts which upon decomposition at high temperatures would yield carbon in the range of 2 – 9 wt % with respect to the ceramic. A dispersant, sodium polyacrylate (NaPAA) (1ml/100gm of ceramic powder) and an antifoaming agent, n-octanol (100µl/100gm (powder basis) were added to the slurries. Zirconia grinding media (2 – 3 mm diameter.) at 1:1 alumina clay to grinding media ratio was added to the slurries contained in a polypropylene bottle and milled on a pot mill for about 24 hours.

Alumina-clay-carbon composites were prepared by slip casting the slurries in ring shaped plastic molds placed on gypsum base plates. Inner surface of the plastic molds was coated with WD40 (WD Company) to reduce adhesion of cast body to the molds. Cast samples were removed from the plastic molds after drying in ambient condition for 36 hours followed by drying in an oven maintained at 50^{o}C for 5 days. Sintering of the samples was done in flowing argon atmosphere at 1400^{o}C with initial heating at 2^{o}C/min upto 600^{o}C, followed by a dwell of two hours at 600^{o}C to pyrolyze sucrose and then heating was continued to 800^{o}C at 5^{o}C/min and finally the temperature was raised to 1400^{o}C at 2^{o}C/min followed by furnace cooling. The sintering temperature of 1400^{o}C was selected based on preliminary experiments which suggested that higher density and strength was achieved at 1400°C than the lower sintering temperatures. Thickness and diameter of each sample for electrical and mechanical measurements were 5 mm and 20 mm respectively. Thickness and diameter of each sample of each sample for thermal conductivity measurement were 3 mm and 12.7 mm respectively.

2.2 Materials Characterization

To see the effect of increasing amount of sucrose addition on the viscosity of the slurries, rheology measurement was done using concentric rheometer cup (DG 26.7/Q). Viscosity of the slurries was measured at a constant shear rate of $10s^{-1}$. Sintered samples were characterized by field emission scanning electron microscopy (JEOL,JSM-7600F). Specific resistance of the sintered samples made by addition of carbon black and sucrose was measured using broadband dielectric spectrometer (Novo control technologies Germany, Concept 80) at 55Hz and also measured for composites made using sucrose in the frequency range of 1Hz to 10^5Hz at room temperature. Carbon retained in sintered alumina-clay-carbon composites made using sucrose as the carbon precursor was measured by thermo gravimetric analysis (SDTA 851Mettler-Toledo system) in the temperature range from room temperature (25°C to 900°C). Carbon produced independently (without the ceramic matrix) from the graphitization of sucrose at 1400^0C was characterized by FEG-SEM (JEOL,JSM-7600F), FEG-TEM (JEOL,JEM- 2100F), BET (Smart Sorb 92/93, Smart Instruments Co.), DLS (Beckman Coulter, Delsa Nano C particle analyzer), XRD (Expert Pro, 40kV, 30mA, Panalytical) and Raman spectroscopy Jobin-Yvon, France Ramnor HG-2S Spectrometer).

Raman spectroscopy measurement of the sintered samples was done by using laser Raman spectrometer (Jobin-Yvon, France Ramnor HG-2S Spectrometer).Phase analysis of sintered samples was done by XRD (Expert Pro, 40kV, 30mA, Panalytical). Thermal conductivity of the composites was determined from thermal diffusivity, specific heat capacity and density measured independently. Thermal diffusivity of the sintered samples was measured by Thermal diffusivity meter (LFA 467 Hyper Flash) from 50°C to 275°C. Specific heat capacity of the sintered samples was measured by differential scanning calorimeter (Q 200,TA instruments) from 50°C to 275°C.Density of the sintered samples was measured by Archimedes principle. Crushing strength of the sintered samples was measured using a UTM (Universal testing machine, Tinius Olsen, UK).

3. Results and discussion

Sucrose added to the alumina-clay slurries as a soluble source of carbon enhanced fluidity of the slurries. It was observed that increasing amount of sucrose addition caused almost no increase in viscosity until an addition of 7 wt % (carbon equivalent). The fact that the viscosity remained constant despite decrease in water amount indicated that sucrose played a role in countering the effect of reduced water content. The above observations can be seen in light of the observations by Pradhan et. al [34] where in addition of sucrose apparently resulted in weakening of the inter-particle network. This weakened inter particle network was ascribed to the enhanced steric hindrance because of the presence of sucrose molecules in association with polyacrylate molecules adsorbed on alumina-clay particles surfaces. Also, it was observed by DLS measurements that as the amount of the sucrose in the slurries increased the particle size (secondary particle size) decreased from 1.2μm for sucrose addition of 2 wt % carbon equivalent to 0.96 μm for sucrose addition of 9 wt % carbon equivalent.

Alumina-clay-carbon composites prepared by slipcasting as described above were porous with porosity increasing with increasing sucrose addition. The sample without sucrose addition showed an open porosity of 10 % and the open porosity increased with addition of sucrose from 15% for the samples with 2 wt% carbon content to 29% with 9 wt% carbon content. The increase in porosity with increase in sucrose addition must have been caused by inhibition of densification of the composites by presence of fine and uniformly dispersed carbon produced from the graphitization of sucrose. Carbon particles produced from the graphitization of sucrose are not expected to sinter to each other and rather they resulted in poorer packing and contact between alumina-clay particles restricting densification. Carbon particles formed in-situ from decomposition of sucrose over the entire alumina-clay powder surface must be extremely fine that though they were not visible in the SEM micrographs (Fig. 2) but elemental mapping confirmed the uniform distribution of carbon in sintered samples (Fig. 3).

The presence of carbon in the sintered samples was also confirmed by other characterization techniques. The proof of uniform distribution of carbon in sintered samples came from Raman spectroscopy carried out over polished sample surfaces at five different locations well separated from each other. Raman spectra collected from the five different locations on representative composite samples with 2, 5, 7, and 9wt% (carbon equivalent) sucrose addition respectively showed presence of carbon with prominent peaks at 1347 and 1598 cm^{-1} as shown in figure 4. The I_D /I_G ratio for 2wt% and 9wt% was 1.24 and 1.22 indicating formation of defective graphitized carbon. As discussed later, the defective nature of carbon formed here (turbostratic graphite) was also suggested by XRD as well. The intensity of the peaks in the 9wt% sample was high compared to the 2wt% sample as shown in figure 5. This may be due to more amount of graphitized carbon present in 9wt% sample. The presence of clay in composite may have played two roles - one as an inorganic binder to bind alumina particles and another to form in-situ mullite crystals and free silica (cristobalite low) crystals as shown in XRD (Fig.5) which is expected to contribute to strengthening of the body. Alumina phase was also confirmed by XRD pattern (Figure 5). The broad peak between 8^o-19^o (2θ) in indicated presence of amorphous metakaolinite resulting from calcination of clay [35]. Metakaolinite contains a highly disordered structure with the remnants of Si-O networks [36].

The presence of carbon in sintered samples was further confirmed by TGA analysis of the crushed composite samples though the weight loss attributable to loss of carbon by combustion was lower than expected as per the amount of sucrose added. As shown in figure 6, the actual amount of carbon that must have been incorporated into the composite samples from graphitization of sucrose was equivalent to around 30 – 40 % yield. For example, around 0.84 wt% carbon was found in samples with sucrose addition of 2wt% equivalent carbon and 3.10 wt% for samples with sucrose addition of 9wt% equivalent carbon. The lower weight loss seen in TGA or lower amount of carbon incorporated in composites could be due to loss of some amount of carbon during the sintering step though it is carried out in flowing argon.

It is believed that the sucrose molecules as present in the slurries used for preparing composites would be present as adsorbed molecules on particles throughout the green dried body. The adsorbed sucrose molecules remain isolated from each other and during heat treatment convert to much finer carbon particles as compared to when the sucrose alone is pyrolyzed. In contrast to the formation of fine uniformly dispersed carbon particles in the composites which were difficult to image, sucrose when pyrolyzed in isolation (in absence of the ceramic) formed large aggregates composed of fine carbon particles (Figure 7). Higher magnification micrographs indicated that the individual flakes were composed of much finer particles as also confirmed by TEM (figure 8). FEG-TEM of carbon particles appeared to be slightly finer (figure 8) in size (25 nm). The agglomeration of the particles appeared to be much more severe. The diffraction pattern shows the polycrystalline nature of the particles. BET surface area analysis (Smart Sorb 92/93, Smart Instruments Co.) of carbon produced by sucrose was found to be 8 m^2/g and DLS particle size analysis (d_{50}) was found to be 1170 nm. Both the results were also confirmed by SEM analysis. The carbon produced was crystalline as seen from the XRD results (Fig. 9). The XRD pattern shows two peaks corresponding to the crystalline reflections from (002) and (103) planes. The 2Theta values at which the intensity maximum was observed for (002)/(103) planes are

24.23/43.45.The interplanar (d-spacing) calculated from Bragg equation for carbon produced by sucrose is 2.35 A^0. It is clear that the carbon prepared from sucrose has turbostratic graphite structure [37-38]. The ratio (I_D /I_G) for the carbon produced from pyrolysis of sucrose in absence of ceramic was 1.09 as shown in figure 10. An increase in I_D/I_G ratio for carbon formed in-situ in composite as reported in this study may be due to an increase in defect density in carbon structure produced from the graphitization of sucrose in composite [39].

The observation that sucrose pyrolysis must have resulted in fine carbon particles distributed uniformly throughout the composite samples was also witnessed from the electrical characteristics of the material. Sintered samples obtained from slipcast sucrose containing slurries showed significantly lower specific resistance as compared to the sintered ceramic samples without any sucrose addition. Also, the composite samples prepared from sucrose showed much lower specific resistance as compared to composite samples prepared using carbon black particles of equivalent carbon amount. Samples with 2 wt % carbon black showed 7 orders of magnitude higher specific resistance as compared to samples with sucrose addition of 2 wt % carbon equivalent as shown in figure 11. This drastically higher specific resistance for carbon black (BET equivalent particle size 270 m^2/g, TEM size 4nm) was possibly due to the well known challenges encountered in deagglomerating and uniform distribution of carbon black particles in the composite. In contrast use of soluble source of carbon simplified the process of achieving uniform distribution of fine carbon particles thus achieving low specific resistance for the lowest amount of sucrose added in the slurries. It was also observed from the measurements done for soluble carbon source samples in the frequency range of (1Hz- 10^5 Hz) that all composites showed the resistor behaviour as shown in figure 12. Specific resistance in composites from 2wt% to 9 wt% carbon content produced from the graphitization of sucrose decreased as the amount of the carbon content increased. The percolation threshold was achieved even for the lowest amount of sucrose added (2 wt% carbon equivalent) due to homogeneous dispersion of carbon formed from pyrolysis of sucrose and the fact that sucrose was distributed uniformly owing to its solubility in the aqueous medium during slurry preparation. As mentioned earlier, the actual amount of carbon in the sintered sample was possibly lower than 2 wt % yet it resulted in exceptionally low specific resistance. Such low specific resistance in the range of 30 Ohm-cm at less than 2 wt % carbon (as per TGA data) would not have been achieved but for uniform distribution of fine carbon particles. Additionally, it is likely that the in-situ carbon obtained from sucrose in the composites was ultrafine (in the nm range) thus leading to lower inter-particle spacing and thus formation of a contiguous network at low weight percent. These results can be viewed in reference to the results reported for different alumina-clay-carbon composites, for example, for a 1.16 vol % CNTs in alumina the specific resistance was much higher at 250 Ohm-cm [28] and for a composite with in-situ generated carbon in gelcast alumina samples with 10.75 wt % carbon equivalent of MAM-MBAM the specific resistance was found to be around 2 Ohm-cm [29]. It is thus clear that results obtained in the present study were better or matched with the results reported in literature for similar carbon contents.

Since at the initiation of the present work the expectation for the amount that will result in percolation was unknown, 2 wt % carbon equivalent was chosen as the lowest amount. Experiments were carried out for even lower sucrose amount addition and it was found that percolation was achieved for 1wt% carbon equivalent sucrose addition as well.

While increase in carbon would have been expected to contribute towards improvement in thermal conductivity but the increase in porosity with increasing sucrose addition dominated and resulted in lowering of thermal conductivity. Alumina-clay-carbon composite with 2 wt% carbon content showed higher thermal conductivity while ceramic carbon composite with 9wt% carbon content showed lower thermal conductivity. Increase in porosity also resulted in lowering of crushing strength of the samples prepared with higher sucrose additions as shown in figure 13.

4. Conclusions: Alumina-clay-carbon composites were prepared by dispersing carbon black in alumina-clay as well as by generating in-situ carbon using sucrose as the soluble source of carbon. Use of sucrose as the source for carbon resulted in samples with uniform distribution of ultrafine carbon leading to percolation being achieved at carbon content less than 1 wt %. Sucrose addition of 2 wt % (equivalent carbon) resulted in drastically lower resistivity (30 Ohm-cm) as compared to that achieved with 2 wt % carbon black (10^8 Ohm-cm) owing to challenges in dispersion of carbon black (BET 270 m^2/g). The samples produced using 2 wt % (equivalent carbon) sucrose addition had modest compressive strength (~ 341 MPa). Overall, use of sucrose as the source of carbon made the processing of low resistivity alumina-clay-carbon composites relatively easy suggesting that the process can be used for applications such as manufacturing of high voltage resistor industrially.

Acknowledgement

The authors are grateful to SAIF, IIT Bombay.

References

[1] http://www.hvrint.com
[2] Takahashi, M., Adachi,K., Ruben L., Menchavez, M., Fuji, J. Mater. Science 2006, 41, 1965–1972.
[3] Shao, Z., Haile, S., M. A Nature 2004, 431,170-173.
[4] Tatami, J., Katashima,T., Komeya, K., Meguro, T., Wakihara, T., J. Am. Ceram. Society 2005, 88, 2889–2893.
[5] Capkova, P., Matejka,V., Tokarsky, J., J. Euro. Ceram. Society 2014, 34, 3111–3117.
[6] Ahmad, K., Pan, Wei., Shi, Sui-Lin., Appl.Phys.Letters 2006, 89, 133122 (1-3)
[7] Goor, Gi., Sagesser, P., Berroth, K., Solid State Ionics, 1997, 101-103, 1163-1170.
[8] Kanbara, T., Yamamoto, T., J. Mat. Sci. Letters, 1987, 6, 1195-1197.
,[9] Cho, J., Boccaccini, A.R., Shaffer, M. S. P., 2009, 44, 1934–1951.
[10] Kumari, L., Zhang, T., Du, G.H., Li, W.Z., Wang, Q.W., Datye, A., Wu, K.H., Ceram. International 2009, 35, 1775–1781.
[11] Fan,BZ., Liu, L., Li, J., Song,J., Chen, J., Shi, J., Zhai. Carbon 2003, 41, 1309-1328.
[12] Lewis, J., A. J. Am. Ceram. Society 2000, 83, 2341–2359.
[13] Jean, G., Sciamanna, V., Demuynck, M., Cambier, F., Gonon M., Ceram. International 2014, 40, 10197–10203.
[14] Bertrand, G., Roy, P., Filiatre, C., Coddet, C., Spray-Dried Ceramic Powders Chem. Eng. Science 2005, 60, 95 – 102
[15] Combe, E., Guilmeau, E., Savary, E., Cloots, R., Funahashi, R., Boschini F., J.Euro. Ceram. Society 2015, 35, 145-151.
[16] Takao, Y., Hotta, T., Naito, M., N., Shinohara M., Okumiya , K., Uematsud. J. Euro. Ceram. Society 2002, 22 , 397-401.
[17] Menchavez, R. L., Fuji, M., Takegami, H., Takahashi, M., Mater. Letters 2007, 61, 754-756.
[18] Menchavez, R. L., Fuji, M., Takahashi, M., J. Euro. Ceram. Society, 2009, 29, 949-954.
[19] Balazsi, C. S., Konya, Z., Weber,F., Biro, L. P., Arato, P.,. C 2003, 23, 1133-1337.
[20] P. K. T. Liu, R. K. Bergstrom, D. G. Gatty, US Patent 4 795 735, 1989.
[21] Shui, Xi., Chung, D.D.L., Carbon 2001, 39, 1717-1722.
[22] Zhan, G.D., Mukherjee, A. K., Int. J. Appl. Ceram. Technology 2004, 1, 161-171.

[23] Zhan, G.D., Kuntz, J. D., Garay, J. E., Mukherjee, A. K., Appl. Phys .Letters 2003, 83, 1228-1230.
[24] Fan, J., Zhao, D., Wu, M., Xu, Z., Song, J., J.Am.Ceram. Society 2006, 89, 750-753.
[25] Cohen, J., Am. Ceram. Bulletin 38 (1959) 441-446
[26] Palilla, F. C., Macallister, B. W., McKenna, J. F., Am. Ceram. Bulletin 1985, 64, 580-585.
[27] Bondar, Iordache, A. M., I., J. Optoelectron. Adv. Mater. 2006, 8, 631-637.
[28] Rul, S., Lefevre-Schlick, F., Capria, E., Laurent, C., Peigney A., Acta.Mater. 2004,52, 1061-1067.
[29] Menchavez, R. L., Fuji, M., Takahashi M., Adv. Materials 2008, 20, 2345–2351.
[30] Michio, I., Jieshan, Q., Quangui, G., Carbon 2015, 87,128-152.
[31] Akira, K. , Yuto, T., Takashi T., Hidetaka, H.,Mat. Letters,2011,65,2197-2200.
[32] Bernardo, M., Marcos, G., Evgeniy, T., Cor E. K., Gijsbertus de, W.,Pow.Technology,2012,221,351-358.
[33] Menchavez, R.L., Fuji,M., Shirai,T., Kumazawa, T., J. Eu. Ceram. Society, 2014,34,717-729.
[34] Pradhan, M., Bhargava, P., J. Am. Ceram. Society, 2005, 88, 833–838.
[35] Nasser Mostafa, Y.,Mohsen, Q., El-maghraby, A., Int.J. Min.Met.Materials,2014,6,609-619.
[36] Kakali, G., Perraki,T., Tsivilis, S., Badogiannis, E., Appl. Clay Sci., 20(2001), 1-2, 73-80.
[37] Narasimman, R., Prabhakaran,K., Carbon 2012, 50,1999-2009.
[38] Narasimman, R., Prabhakaran ,K.,,Carbon 2012,50,5583-5593.
[39] Arvind Agarwal,Srinivasa Rao Bakshi,Debrupa Lahiri,Carbon Nanotubes Reinforced Metal Matrix Composites

byintering mixtures of carbon and clay

Figure Captions

Figure1. Flow-chart of fabrication of alumina-clay-carbon composite

Figure 2. FEG-SEM micrographs (a&b) of alumina-clay composite, (c) of alumina-clay-carbon composites with 2 wt % (15% open porosity) (d) with 5 wt % (18% open porosity) (e) with 8 wt % (26% open porosity) (f) with 9wt% carbon content (29.% open porosity) produced by graphitization of sucrose sintered at 1400^{o}C.

Figure 3. Elemental mapping of alumina-clay-carbon composites, (a) alumina-clay-carbon composite with 2wt% carbon and (b) alumina-clay-carbon composite with 9wt% carbon sintered at 1400^{o}C . The red dots represent the uniformly distributed sucrose derived carbon in the samples.

Figure 4. Raman spectra of alumina-clay-carbon composites containing 2, 5, 7, and 9wt% carbon (2S, 5S, 7S, 9S) as expected from sucrose graphitization following sintering at 1400^{o}C

Figure 5. XRD analysis of alumina-clay-carbon composites (2 and 9wt % carbon content – 2S, 9S) sintered at 1400^{o}C

Figure 6. TGA of the alumina-clay-carbon composites sintered at 1400°C with ceramic matrix composed of 35 wt % alumina-65 wt % clay for 2, 5, 7, and 9 wt% carbon content (2S, 5S, 7S, 9S) as expected from graphitization of sucrose

Figure 7. (a) FEG-SEM micrographs of carbon flakes produced by sucrose graphitized at 1400°C (b) Higher magnification view of an individual carbon flake showing that individual flakes were composed of nanosized carbon particles

Figure 8. FEG-TEM micrograph of carbon produced by sucrose graphitized at 1400°C, (a)&(b) at low magnification, (c) at high magnification and (d) diffraction pattern

Figure 9. XRD pattern of carbon produced from sucrose graphitized at 1400°C

Figure 10. Raman spectra of carbon produced from sucrose graphitized at 1400°C

Figure 11. Specific resistance vs different carbon content of the alumina-clay-carbon composites sintered at 1400°C with ceramic matrix composed of 35 wt % alumina-65 wt % clay for different carbon black content and carbon content produced by graphitization of sucrose

Figure 12.Specific resistance vs frequency of the alumina-clay-carbon composites sintered at 1400°C with ceramic matrix composed of 35 wt % alumina-65 wt % clay for different carbon content produced by graphitization of sucrose

Figure 13. Thermal conductivity, crushing strength vs density of the alumina-clay- carbon composites sintered at 1400^{o}C with ceramic matrix composed of 35 wt % alumina-65 wt % clay for different sintered densities (corresponding to different carbon content produced by graphitization of sucrose).

Figure1

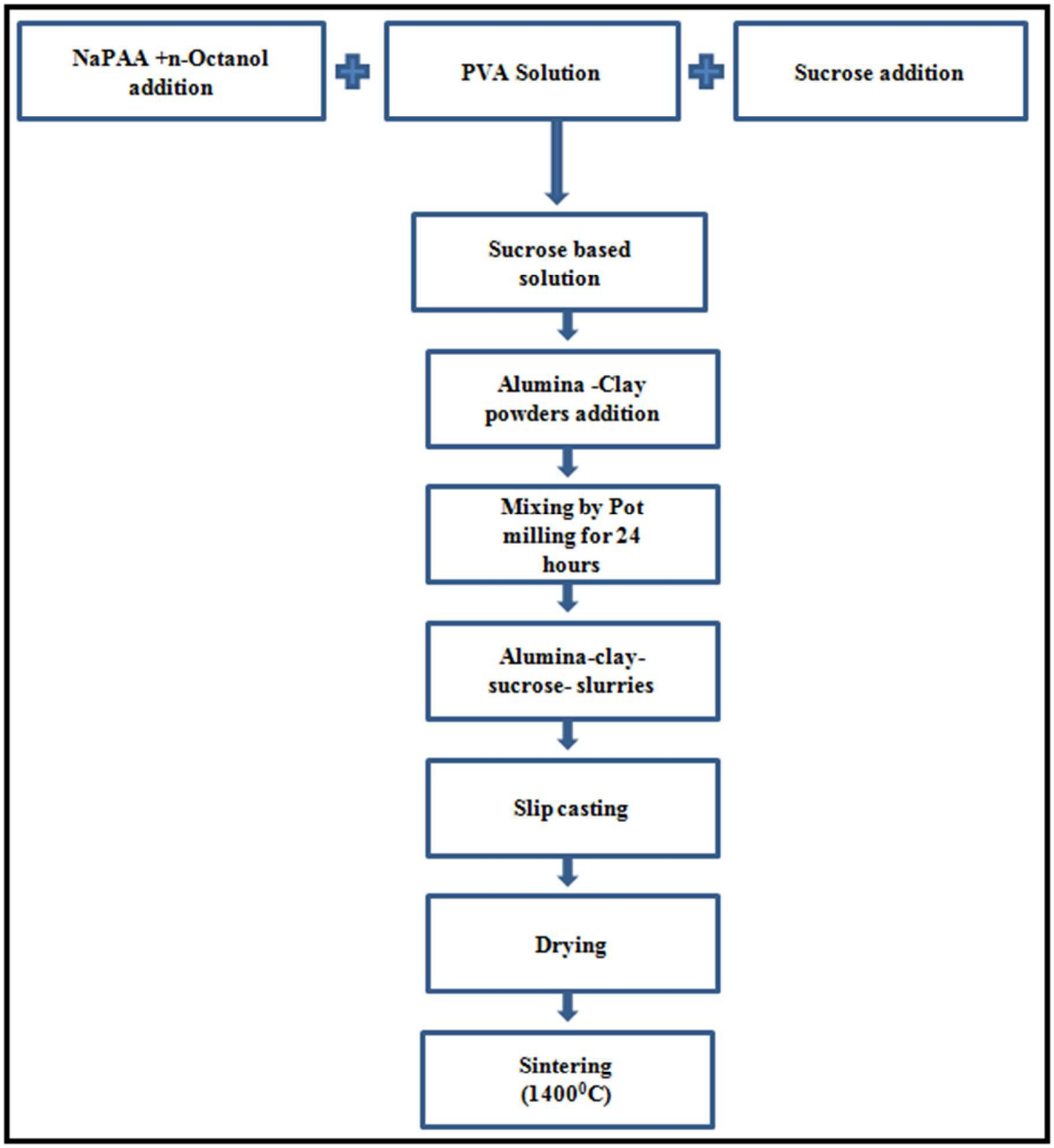
NaPAA +n-Octanol addition
PVA Solution
Sucrose addition
Sucrose based solution
Alumina -Clay powders addition
Mixing by Pot milling for 24 hours
Alumina-clay-sucrose- slurries
Slip casting
Drying
Sintering (1400⁰C)

Figure 2

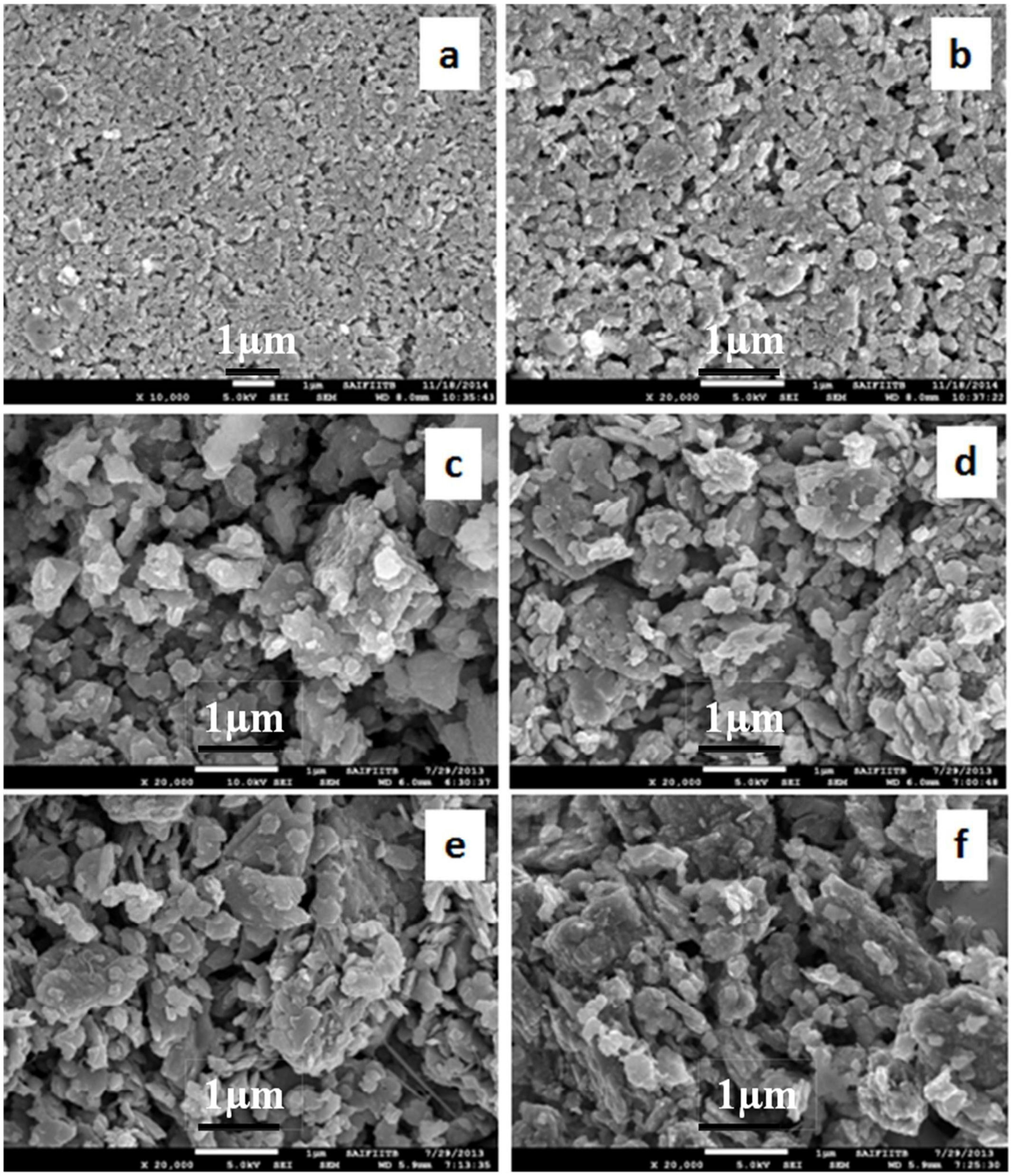
a
1µm
1µm SAIFIITB 11/18/2014
X 10,000 5.0kV SEI SEM WD 8.0mm 10:35:43
b
1µm
1µm SAIFIITB 11/18/2014
X 20,000 5.0kV SEI SEM WD 8.0mm 10:37:22
c
1µm
1µm SAIFIITB 7/29/2013
X 20,000 10.0kV SEI SEM WD 6.0mm 6:30:37
d
1µm
1µm SAIFIITB 7/29/2013
X 20,000 5.0kV SEI SEM WD 6.0mm 7:00:48
e
1µm
1µm SAIFIITB 7/29/2013
X 20,000 5.0kV SEI SEM WD 5.9mm 7:13:35
f
1µm
1µm SAIFIITB 7/29/2013
X 20,000 5.0kV SEI SEM WD 5.9mm 7:25:30

Figure 3(a)

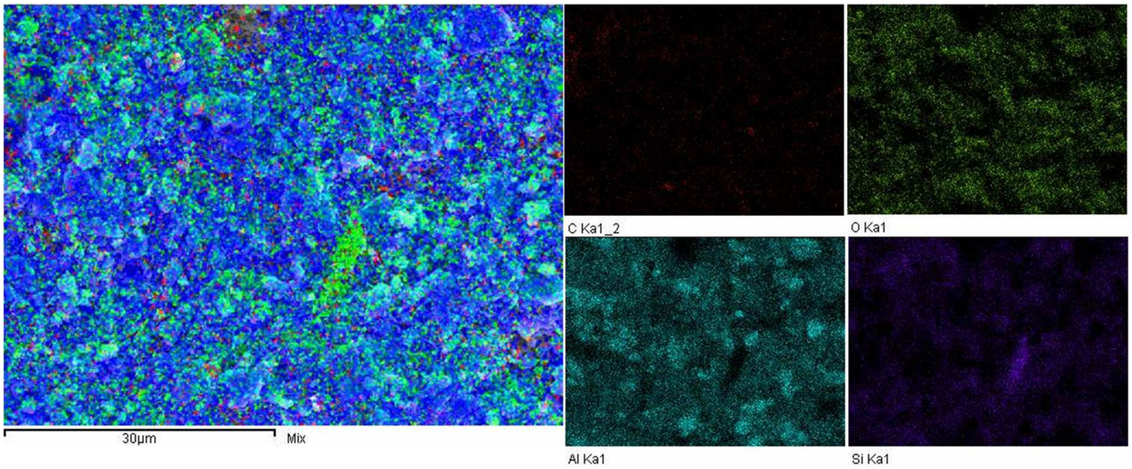

Figure 3(b)

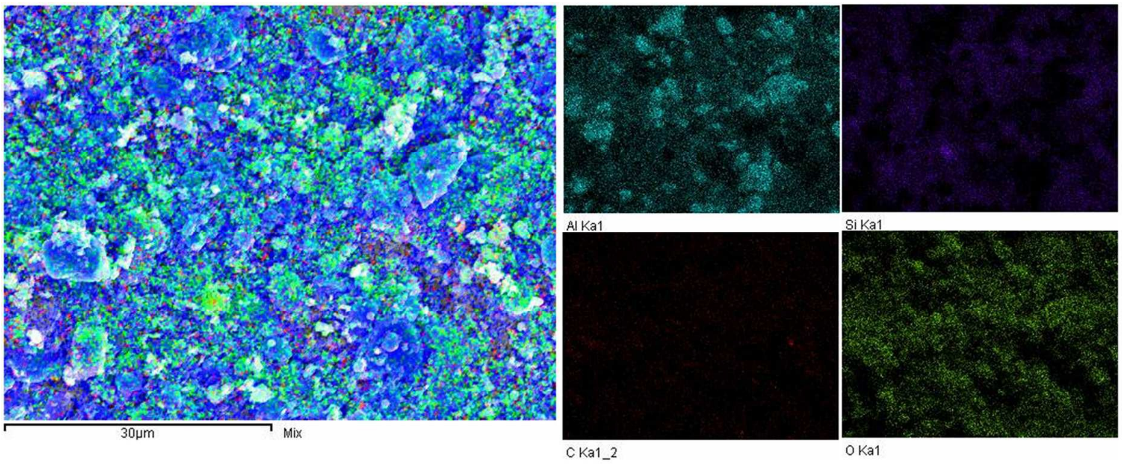

Figure 4

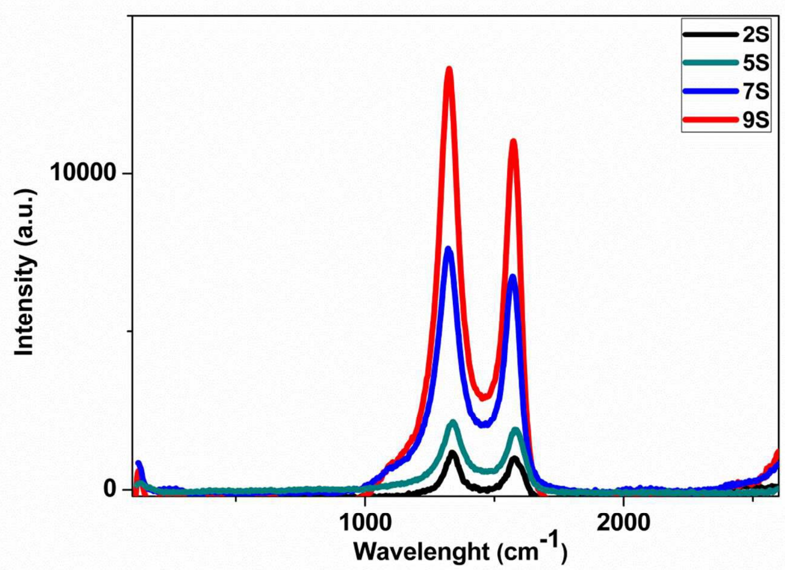

Figure 5

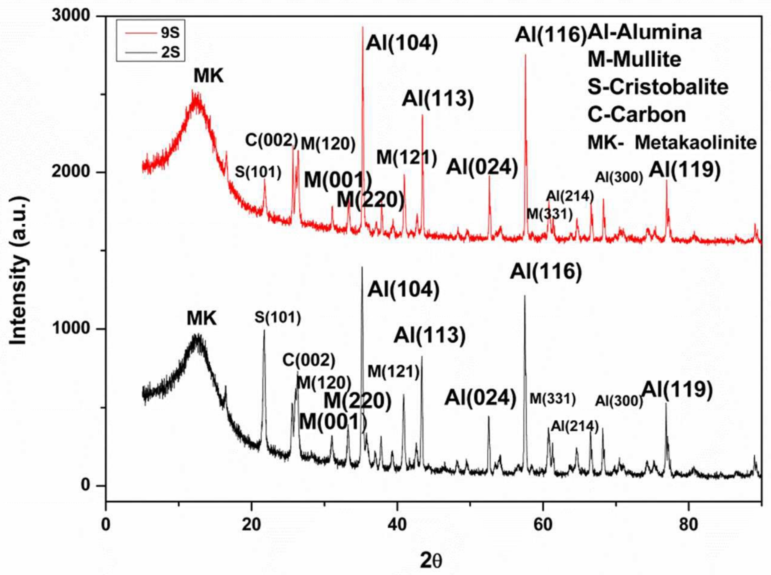

Figure 6

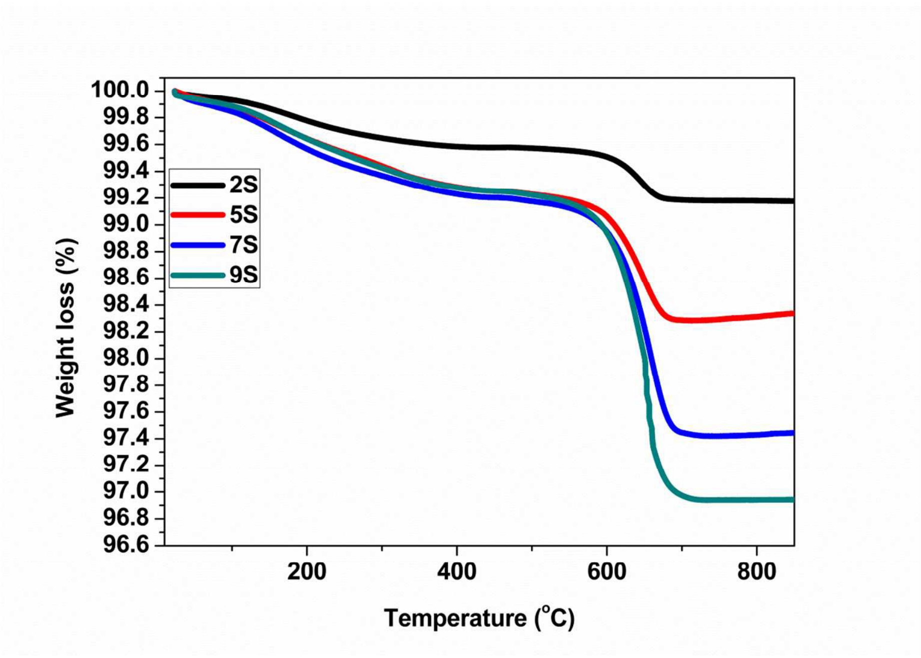

Figure 7

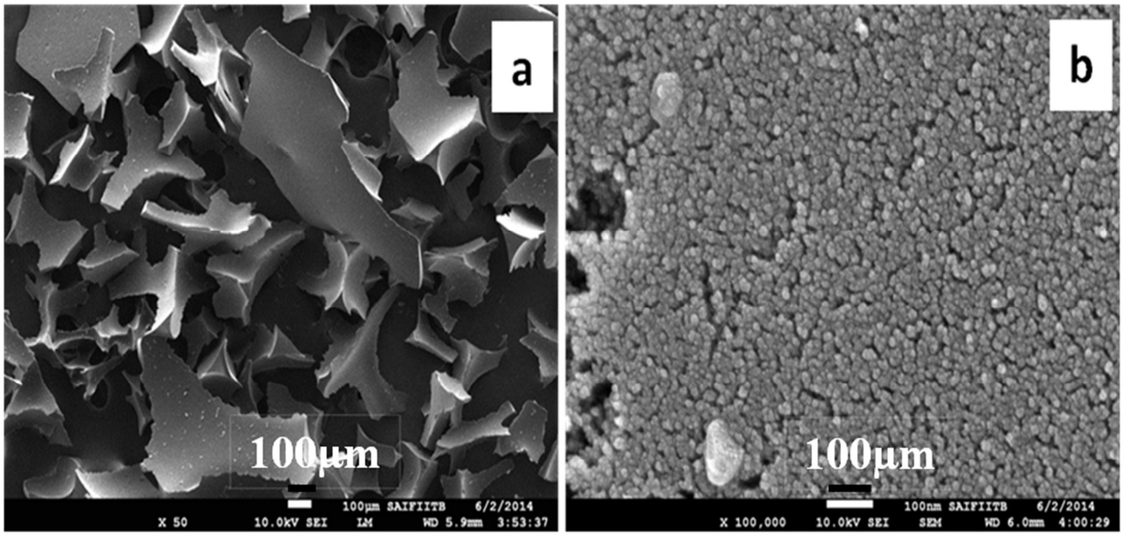

Figure 8

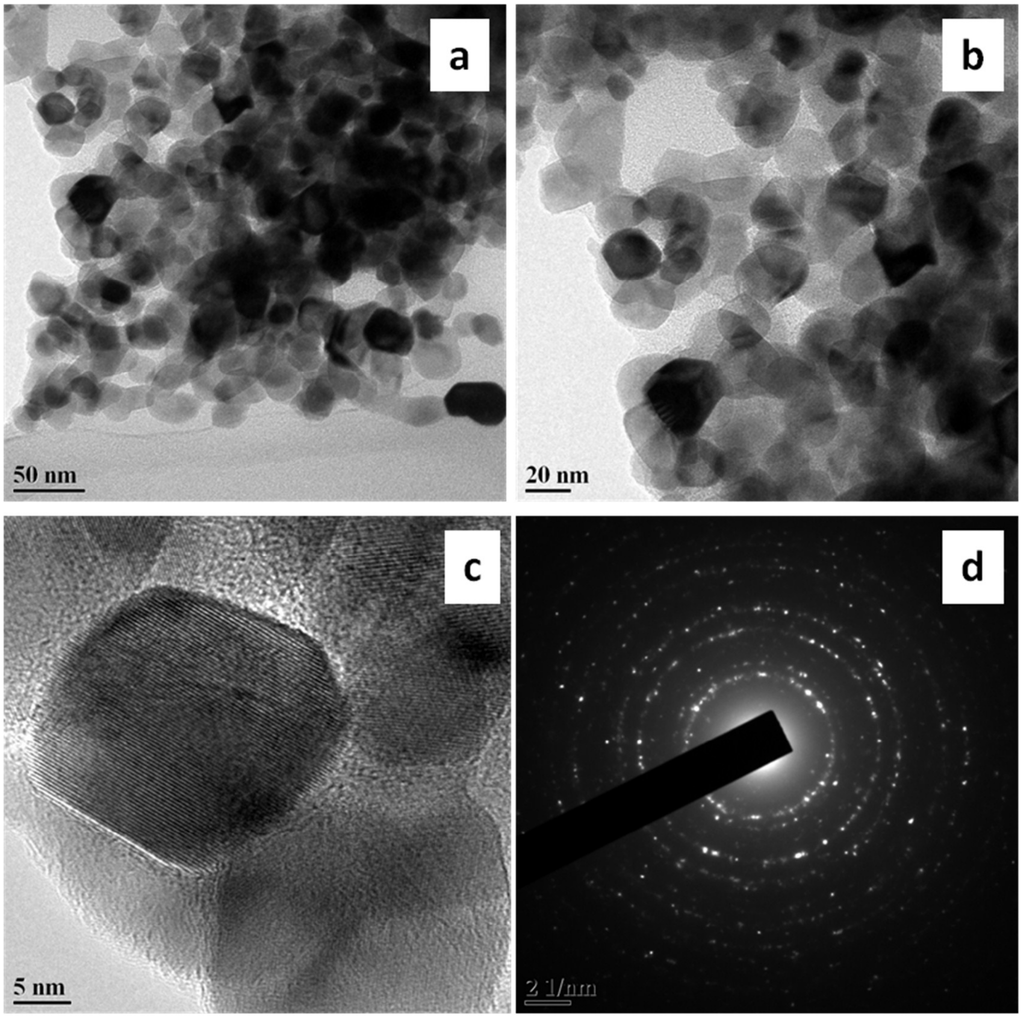

‘

Figure 9

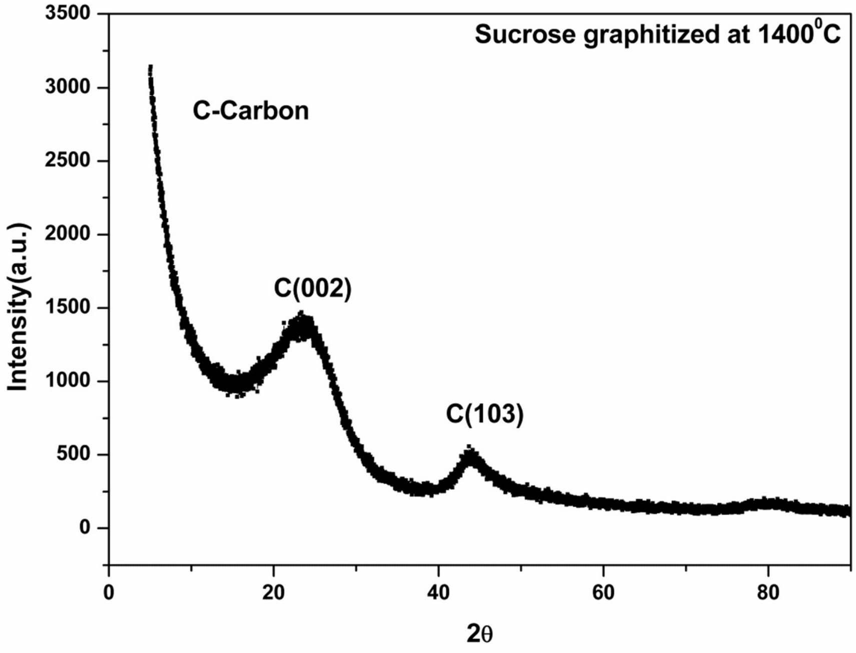

Figure 10

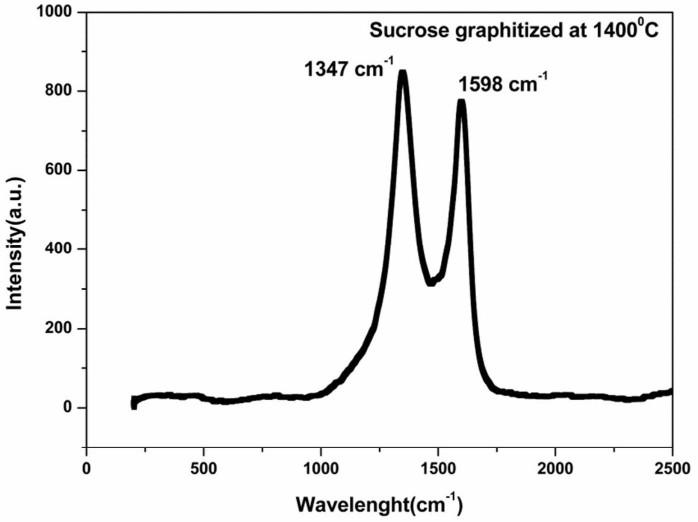

Figure 11

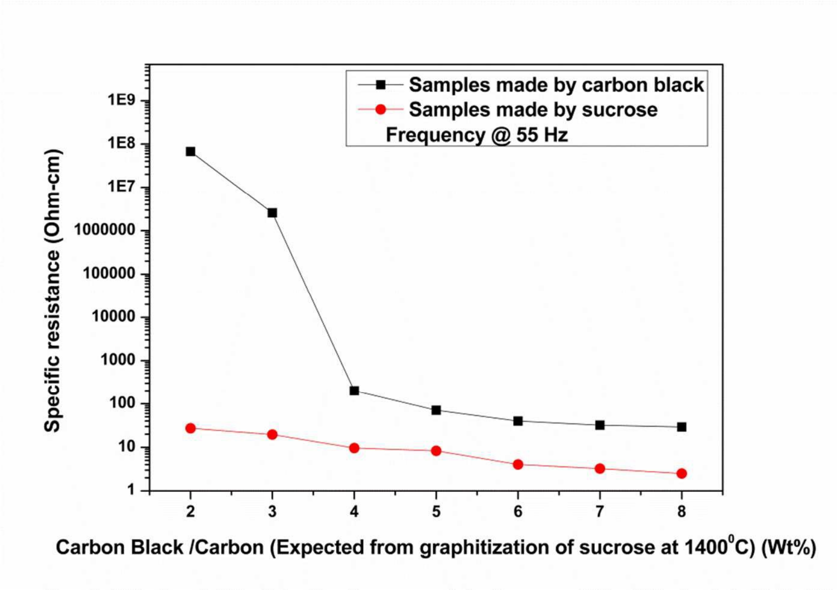

Figure 12

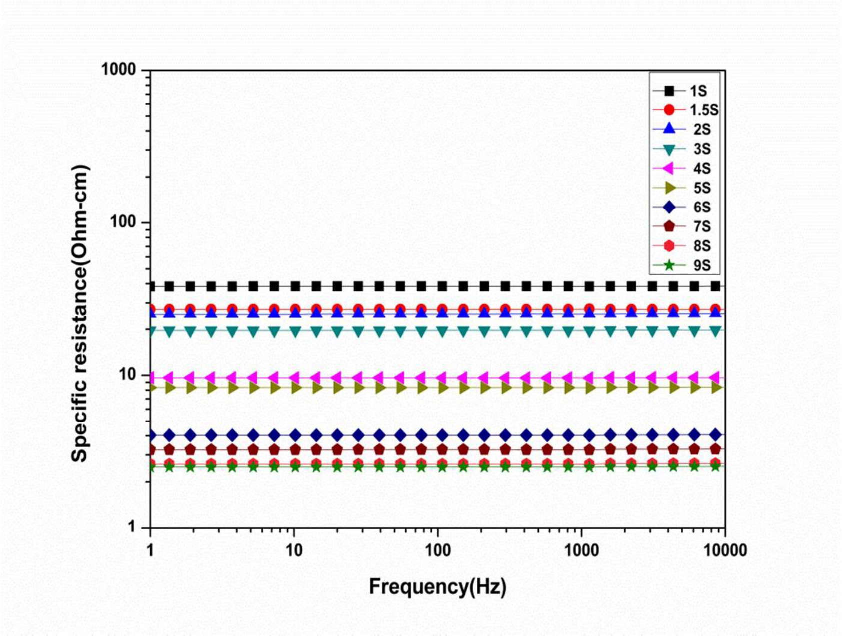

Figure 13

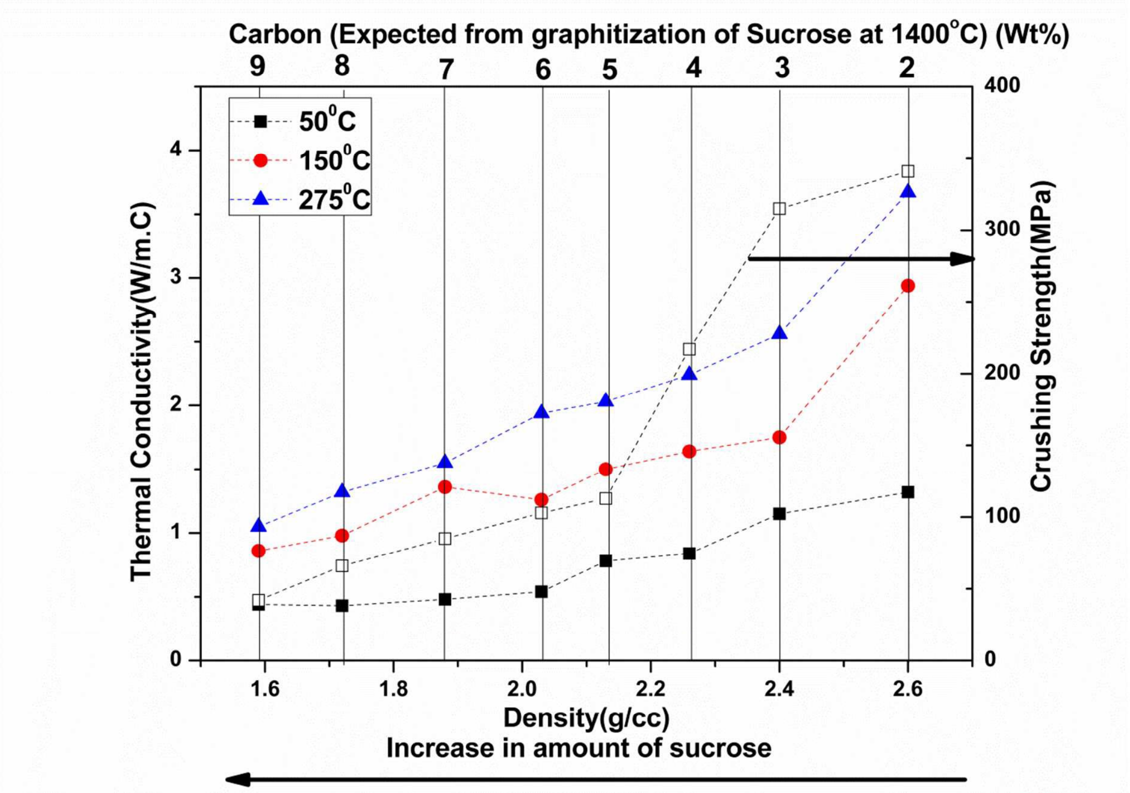
Carbon (Expected from graphitization of Sucrose at 1400°C) (Wt%)
9
8
7
6
5
4
3
2
50°C
150°C
275°C
Thermal Conductivity(W/m.C)
0
1
2
3
4
Crushing Strength(MPa)
0
100
200
300
400
1.6
1.8
2.0
2.2
2.4
2.6
Density(g/cc)
Increase in amount of sucrose

Graphical abstract for review

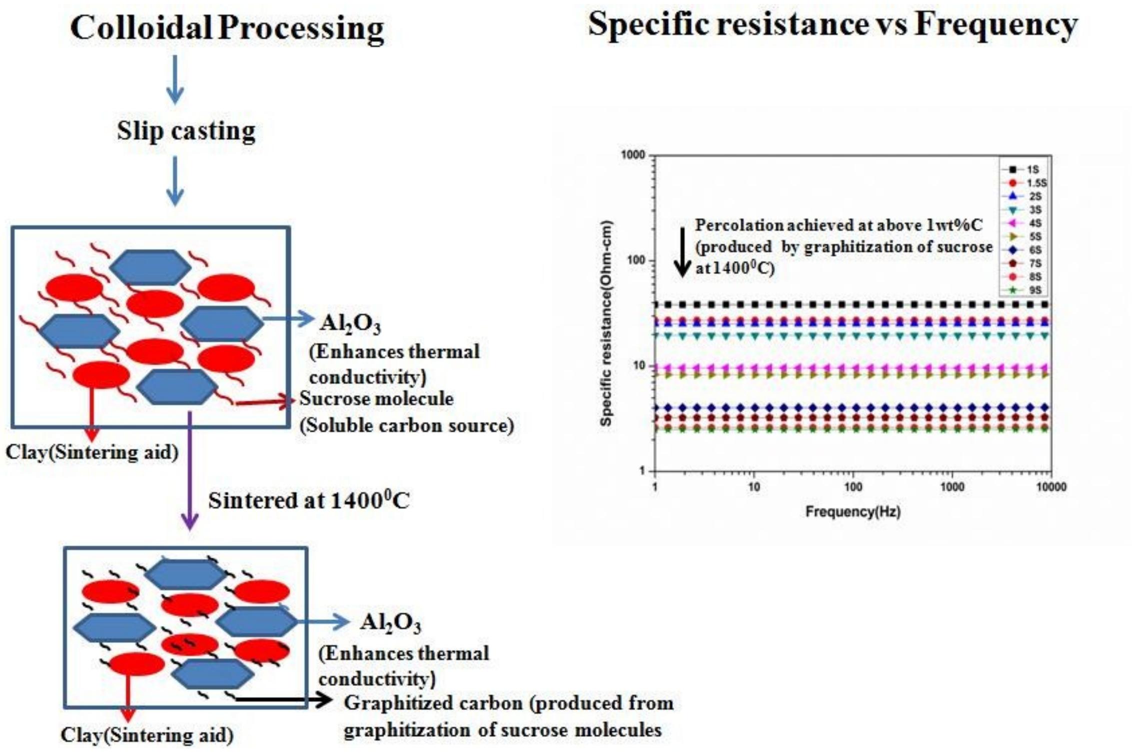

‘